Int. J. Radiation Oncology Biol. Phys., Vol. 61, No. 5, pp. 1551–1558, 2005

0360-3016/05/$–see front matter

ELSEVIER

doi:10.1016/j.ijrobp.2004.12.013

PHYSICS CONTRIBUTION

THE CORRELATION BETWEEN INTERNAL AND EXTERNAL MARKERS FOR ABDOMINAL TUMORS: IMPLICATIONS FOR RESPIRATORY GATING

David P. Gierga, Ph.D.,* Johanna Brewer, B.S.,† Gregory C. Sharp, Ph.D.,* Margrit Betke, Ph.D.,† Christopher G. Willett, M.D.,* and George T. Y. Chen, Ph.D.*

*Department of Radiation Oncology, Massachusetts General Hospital, Boston, MA; and †Department of Computer Science, Boston University, Boston, MA

Purpose: The correlation of the respiratory motion of external patient markers and abdominal tumors was examined. Data of this type are important for image-guided therapy techniques, such as respiratory gating, that monitor the movement of external fiducials.

Methods and Materials: Fluoroscopy sessions for 4 patients with internal, radiopaque tumor fiducial clips were analyzed by computer vision techniques. The motion of the internal clips and the external markers placed on the patient's abdominal skin surface were quantified and correlated.

Results: In general, the motion of the tumor and external markers were well correlated. The maximum amount of peak-to-peak craniocaudal tumor motion was 2.5 cm. The ratio of tumor motion to external-marker motion ranged from 0.85 to 7.1. The variation in tumor position for a given external-marker position ranged from 2 to 9 mm. The period of the breathing cycle ranged from 2.7 to 4.5 seconds, and the frequency patterns for both the tumor and the external markers were similar.

Conclusions: Although tumor motion generally correlated well with external fiducial marker motion, relatively large underlying tumor motion can occur compared with external-marker motion and variations in the tumor position for a given marker position. Treatment margins should be determined on the basis of a detailed understanding of tumor motion, as opposed to relying only on external-marker information. © 2005 Elsevier Inc.

Image-guided therapy, Gating, Fluoroscope, Abdomen, Tracking.

INTRODUCTION

The delivery of highly conformal radiation therapy may be problematic in the presence of respiratory organ motion. For large amounts of respiratory motion, a large planning target volume (PTV) may be required to ensure the delivery of adequate dose to the target. The use of large margins, however, may limit dose delivery because of excessive dose to normal structures. Additionally, for treatment modalities such as intensity-modulated radiation therapy (IMRT), which use a dynamic multileaf collimator (MLC), the motion interplay effect between the MLC motion and the respiratory organ motion may further degrade the tumor dose.

The treatment site of interest for this study is the abdomen. The magnitude of respiration-induced target motion for abdominal tumors may be as large as 2 to 3 cm, peak-to-peak (1–4). The low dose tolerances for normal structures in the abdomen, such as the kidney and liver, however, may limit the use of large treatment margins. For these cases, motion mitigation or compensation techniques may enable smaller treatment margins to be used, which leads to a more conformal treatment and reduces the probability of a geographic miss.

One method that has been proposed to limit the amount of target motion during radiotherapy is respiratory gating (5–11). For implementation of respiratory gating, the motion of an external patient marker is monitored, typically by use of a reflective marker and an infrared camera system. The external marker is used as a surrogate for the tumor motion. One the basis of the motion of the external marker, a gating window can be defined either in terms of the amplitude or in terms of phase. The linear accelerator is then gated off when the external marker moves outside the predetermined window. Respiratory gating relies on the assumption that the motion of the external marker is representative of the motion of the actual tumor motion.

Vedam (12) and Mageras (6) have investigated the correlation between external-marker motion and the diaphragm, a potential surrogate for lung-tumor motion. Their results indicate a generally strong correlation between the diaphragm and external-marker motion. The direct correla-

Reprint requests to: David P. Gierga, Ph.D., Massachusetts General Hospital, Fruit Street, Cox 8, Boston, MA 02114. Tel: (617) 724-2274; Fax: (617) 726-3603; E-mail: dgierga@partners.org

Presented at the 45th Annual Meeting of the American Society for Therapeutic Radiology and Oncology, October 19–23, 2003, Salt Lake City, UT.

Received June 2, 2003 and in revised form Nov 19, 2004. Accepted for publication Dec 3, 2004.

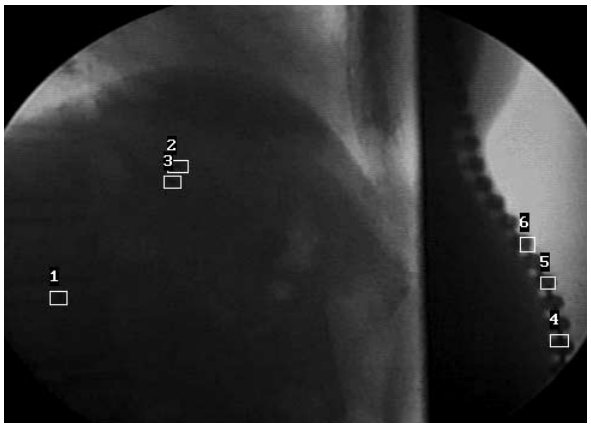

Fig. 1. Lateral fluoroscopic image for Patient 2 at inhale, showing tumor clips (1 to 3) and external markers (4 to 6).

tion between external markers and tumor motion, however, has not been fully studied. Ozhasoglu (13) has published data that show a good correlation of an external marker and a tumor marker for a single pancreas tumor patient, as determined by the Cyberknife tracking system. Our present work aims to more fully quantify the correlation between external respiratory signals and abdominal-tumor motion.

METHODS AND MATERIALS

This study follows the previous work reported by Gierga (14), in which the motion of abdominal tumors (liver and pancreas) was assessed, and the effect of this motion on IMRT treatment plans was estimated. For the current study, data were collected for 4 patients, each with a liver tumor. All of these patients had radiopaque clips placed in the tumor volume for improved localization as part of their normal course of therapy. The number of clips for each patient ranged from 2 to 4. Clips of various sizes were used; clip diameter ranged from 1 to 2 mm and clip length ranged from 4 to 8 mm. Patients were treated with either standard 3D-CRT, IMRT, or proton therapy.

The location of the tumors varied. Patient 1 had a 4-cm mass adjacent to the porta hepatis, approximately 6-cm inferior of the dome of the liver. Patient 2 had a tumor that measured approximately 5 × 3 cm, near the dome of the liver. Patient 3 had a 5-cm tumor in segment VIII of the liver. The tumor for Patient 4 was a 5-cm mass in segment IV of the liver, approximately 4 cm inferior of the dome of the liver.

Motion data were gathered by fluoroscopy during isocenter verification sessions on a conventional simulator. External radiopaque markers were placed on the patient's skin at midline from the xyphoid process to the umbilicus. The fluoroscopic video signal was recorded for about 30 seconds, at a frame rate of 30 frames per second, on a standard video recorder interfaced with the fluoroscopic monitor. Data were taken from the lateral view to allow for simultaneous visualization of both the tumor clips and the external markers. The right-to-left motion of the tumor could be observed from the anterior fluoroscopic view and was typically 1 to 2 mm or less. Any motion in the right-to-left direction (in or out of plane in the lateral view) was neglected when data were collected from the lateral view. Data were gathered under normal, free breathing conditions without any breath control, coaching, or patient instruction. For 1 patient, an abdominal girdle wrap was used to restrict the extent of respiratory motion.

The analog videotapes were converted to a digital video format and then analyzed by computer vision software developed at Boston University (15). The use of this software algorithm to track the motion of tumors is described in greater detail in Gierga (14). The tracking software determines the coordinates of the tumor markers and the external patient markers as a function of time. Tumor-clip motion was tracked in both the craniocaudal and the anteroposterior directions; the magnitude of motion is typically the largest in the craniocaudal direction. The external markers, used to visualize the patient's skin surface, typically move only in the anteroposterior direction. An example screen capture of a lateral fluoroscopic image that shows the tracked tumor clips and external markers is given in Fig. 1. The spatial correlation between the tumor motion and patient's surface-marker motion was then quantified. The frequency characteristics of the data were also examined by using Fourier analysis to transform the data from the time domain to the frequency domain.

RESULTS

The results for the 4 patients are summarized in Table 1. Figure 2 shows the results for Patient 1. Figure 2a shows the craniocaudal motion of 1 clip (i.e., the tumor fiducial marker) and the anteroposterior motion of the external markers as a function of time. The peak-to-peak motion of the clip varied from 0.7 to 1.3 cm, and the external markers moved approximately 3 mm. Marker 1 was most inferior on the patient, and Marker 3 was most superior. Each marker was separated by 18 mm on the patient surface. The anteroposterior motion of the tumor clip for this patient was less than 5 mm (data not shown). Figure 2b shows the correlation between the clip and the 3 external markers. A linear least-squares fit was performed, and the R^2 values ranged from 0.85 to 0.94, depending on marker position. For a

Table 1. Summary of results for four patients

	Patient 1	Patient 2	Patient 3	Patient 4
Maximum craniocaudal tumor motion (cm)	1.3	1.2	2.5	1.3
Maximum anteroposterior tumor motion (cm)	<0.5	1.0	1.2	1.0
Ratio of tumor to external marker motion (craniocaudal direction)	4.1–5.0	1.5–2.4	2.5–7.1	0.85–1.2
Range of tumor position for a fixed marker position (cm)	0.3–0.6	0.2–0.3	0.2–0.4 (2 of 3 markers) 0.9 (1 of 3 markers)	0.2
Breathing period (s)	4.5	3.1	4.5	2.7

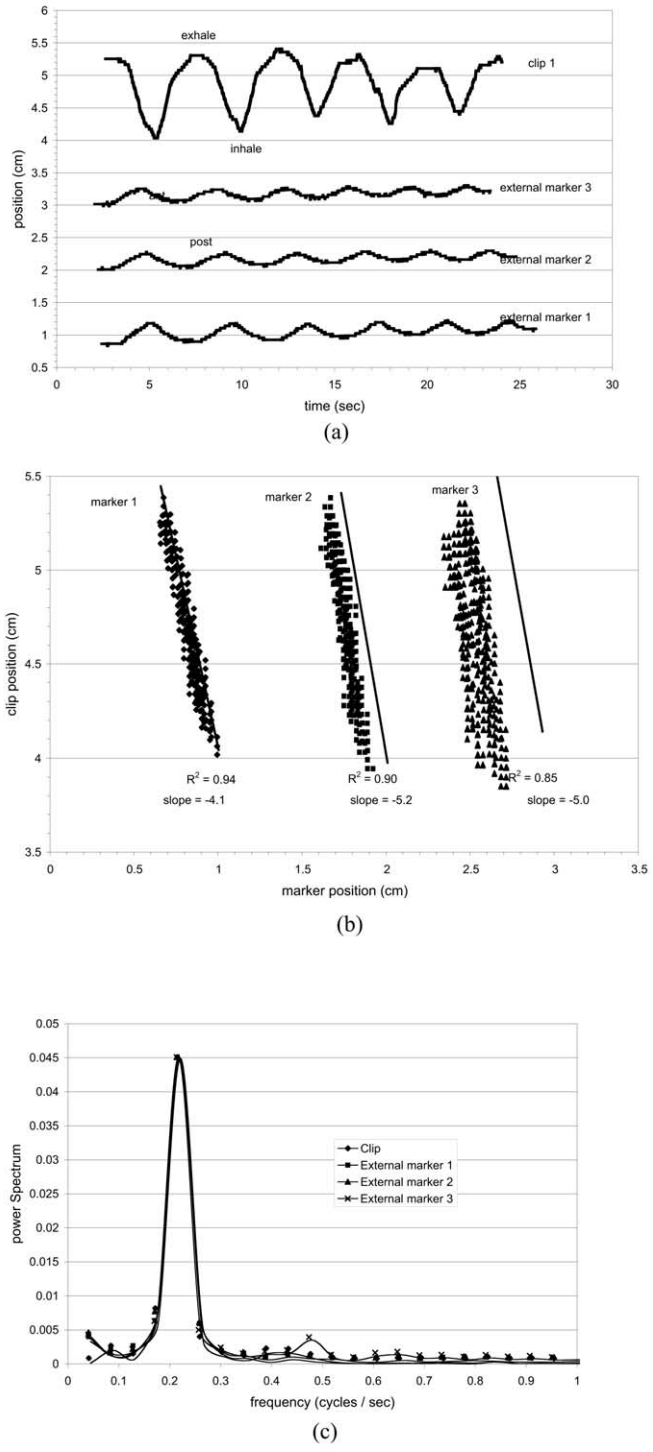

Fig. 2. Patient 1: (a) Craniocaudal tumor clip motion and anteroposterior external-marker motion as a function of time. The absolute values of the motion traces have been modified for display purposes. (b) Craniocaudal tumor clip position as a function of anteroposterior external-marker position. (c) Power spectrum of tumor clip and external-marker motion.

given external-marker position, the range of tumor positions is 3 to 6 mm. The slope values shown in Fig. 2b relate the amount of tumor motion to the amount of external-marker motion. For this patient, the slope values range from a factor of 4 to 5. Figure 2c shows the power series for the clip and the 3 external markers. Each of the fiducials has similar frequency values. A peak frequency of 0.22 cycles per second corresponding to a period of 4.5 seconds.

The motion data for Patient 2 are shown in Fig. 3. A screen capture of a fluoroscopic image at the inhale phase for Patient 2 was shown in Fig. 1. Figure 3a shows the craniocaudal motion of 3 tumor clips and the anteroposterior motion of 3 external markers. Figure 3c shows the corresponding correlation of the position of Clip 3 as a function of external-marker position. The peak-to-peak extent of the craniocaudal tumor motion was 1.0 to 1.2 cm, and the period of motion was 3.1 seconds. Note the region of irregular breathing between 20 and 25 seconds is evident in both the clip and the external-marker motion and does not degrade the correlation shown in Fig. 3c. Figure 3b illustrates the anteroposterior motion of the tumor and external markers, and Fig. 3d shows the correlation between these 2 sets of motion data. For this patient, the anteroposterior tumor motion was about 0.8 to 1.0 cm, nearly as large as the craniocaudal motion. For both directions of tumor motion, the correlation with external marker motion was quite good. Figure 3c and 3d show that the ratio of tumor motion to external-marker motion ranged from 1.6 to 2.4 for the craniocaudal tumor motion and ranged from 1.1 to 1.5 for anteroposterior tumor motion. For Clips 1 and 2 (data not shown), the ratio of tumor motion to external-marker motion ranged from 1.4 to 2.2 for the craniocaudal tumor motion and ranged from 1.0 to 1.7 for anteroposterior tumor motion The tumor position in the craniocaudal direction varied by 2 to 3 mm for a given external-marker position.

Figure 4 shows the motion data for Patient 3. This patient exhibited a large amount of tumor motion, with peak-to-peak motion of 2 to 2.5 cm and 0.8 to 1.2 cm in the craniocaudal and anteroposterior directions, respectively. These large amounts of motion were seen despite the use of an abdominal girdle wrap to restrict the extent of respiratory motion. The breathing period of this patient was 4.5 seconds. Figure 4c and 4d show the motion data for Clip 2 correlated to the external-marker motion. The motion of the tumor was well correlated with the motion of the external markers, but the ratio of craniocaudal tumor motion to external-marker motion ranged from 2.8 to 7.1. For Marker 1, the tumor position in the craniocaudal direction varied by as much as 9 mm for a given marker position. For Marker 3, which had a much lower ratio of craniocaudal tumor motion to external-marker motion, the range of tumor positions for a given marker position was nominally 2 to 4 mm. The external-marker motion was also correlated with the tumor motion from Clip 1 (data not shown). The ratio of craniocaudal tumor motion to external-marker motion for Clip 1 ranged from 2.5 to 6.4. Figure 5 shows the relationship between the craniocaudal and the anteroposterior clip motion for Patient 3. The data are fairly linear, which implies that the craniocaudal and anteroposterior tumor motion are in phase with each other.

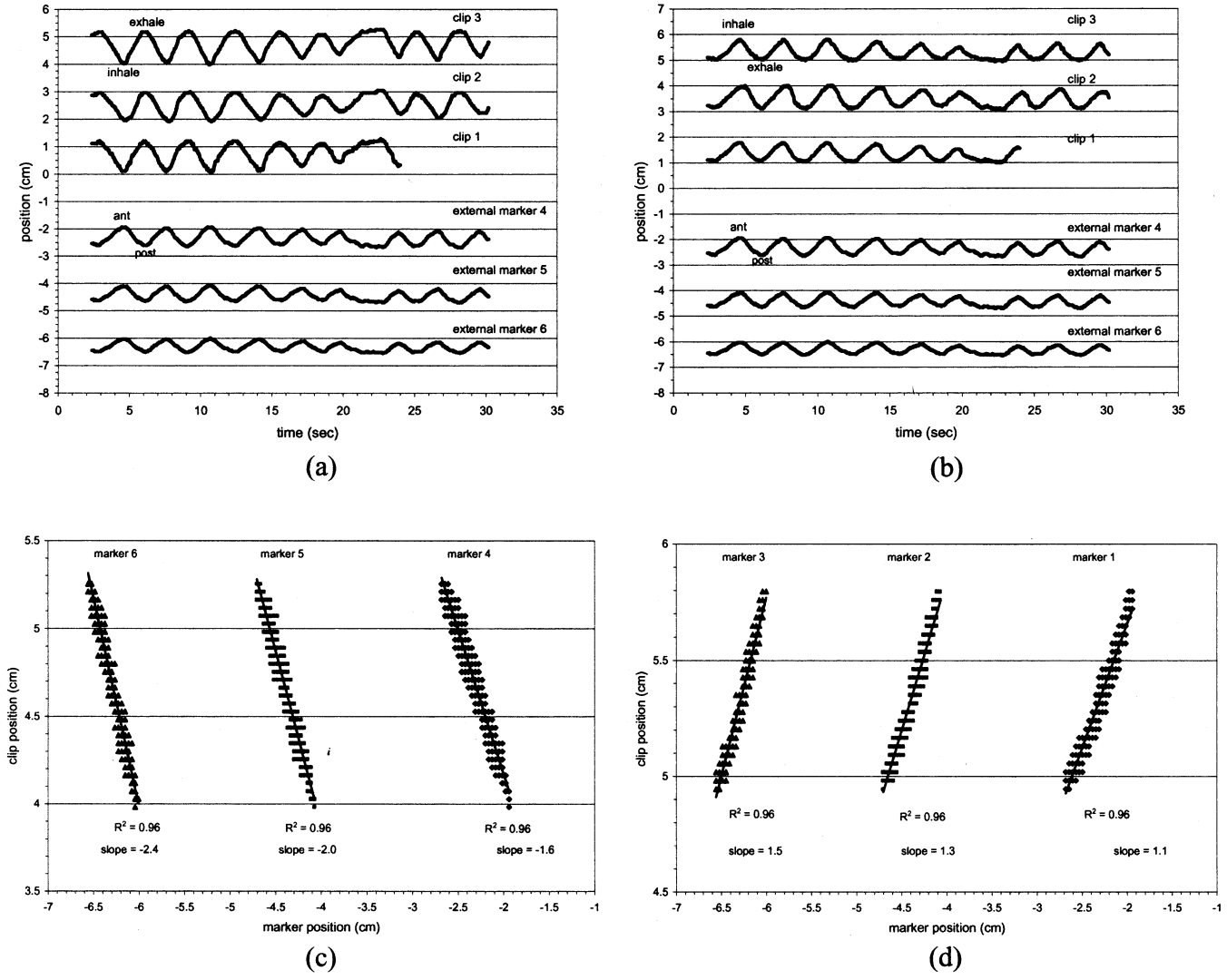

Fig. 3. Patient 2: (a) Craniocaudal tumor-clip motion and anteriorposterior external-marker motion as a function of time. (b) Anteroposterior tumor clip motion and anteroposterior external-marker motion as a function of time. (c) Craniocaudal tumor-clip position (Clip 3) as a function of anteroposterior external-marker position. (d) Anteroposterior tumor-clip position (Clip 3) as a function of anteroposterior external-marker position. For (a) and (b), the absolute values of the motion traces have been modified for display purposes.

The motion data for Patient 4 is shown in Fig. 6. Figure 6a shows both the craniocaudal and anteroposterior motion for tumor Clip 1, as well as the anteroposterior motion of 4 external markers. The peak-to-peak tumor-clip motion was about 1.3 cm in the craniocaudal direction and about 1 cm in the anteroposterior direction. The breathing period of the patient was 2.7 second. The tumor clip and external markers are well correlated (shown in Fig. 6b and 6c). The average ratio of tumor-clip motion to external-marker motion was 1.0 for craniocaudal tumor motion and 0.7 for anteroposterior tumor motion. For each external marker, the tumor positions varied by about 2 mm for a given marker position in the breathing cycle.

For patients with multiple clips, the deformation of the tumor can be examined by plotting the difference in clip positions over time. For rigid-body motion in the lateral plane, the relative spacing of the individual tumor clips would be constant if rotations were neglected. Note that because orthogonal images are not obtained simultaneously, a true 3D model of clip motion cannot be determined. Figure 7 shows the difference in clip positions (i.e., the clip spacing) over time for Patients 2 and 3. The data for Patient 2, who had 3 tracked clips, are shown in Fig. 7a. The difference in clip positions for Clips 2 and 3, relative to Clip 1, are shown for both the craniocaudal and anteroposterior directions. The range in the difference between Clip 1 and Clip 2 is nearly 5 mm, in both directions. The standard deviation of the difference in clip positions, normalized by use of the maximum peak-to-peak amplitude, is 5.5% in the craniocaudal direction and 6% in the anteroposterior directions. The range in the difference of clip positions for Clips 1 and 3 is much smaller, roughly 3 mm. The standard deviation of the clip spacing is less than 2% for both motion directions.

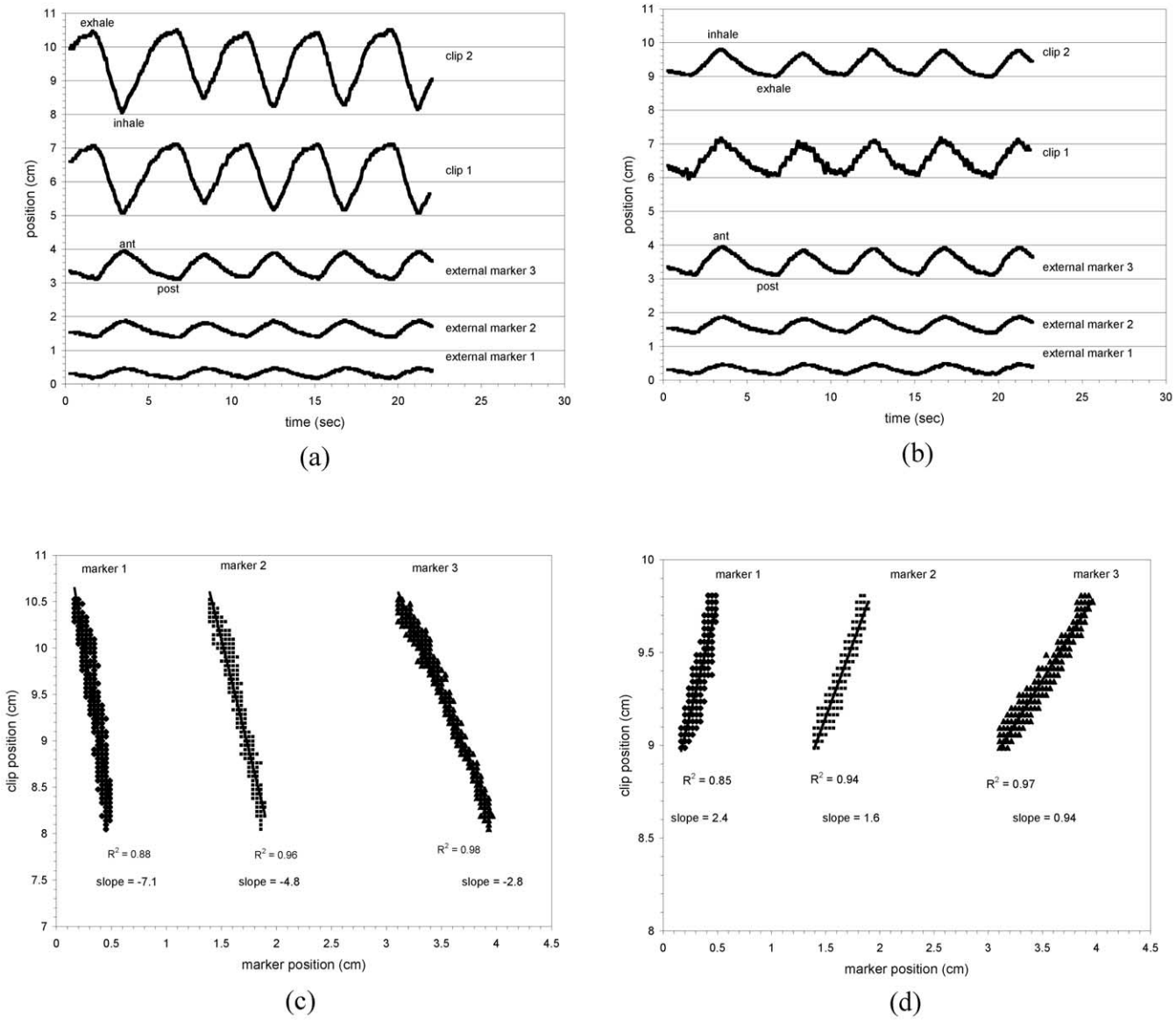

Fig. 4. Patient 3: (a) Craniocaudal tumor-clip motion and anteroposterior external-marker motion as a function of time. (b) Anteroposterior tumor clip motion and anteroposterior external-marker motion as a function of time. (c) Craniocaudal tumor clip position (Clip 2) as a function of anteroposterior external-marker position. (d) Anteroposterior tumor-clip position (Clip 2) as a function of anteroposterior external-marker position. For (a) and (b), the absolute values of the motion traces have been modified for display purposes.

DISCUSSION

For the 4 patients examined in this study, both craniocaudal and anteroposterior tumor motion correlated well with external-marker motion. For these patients, the amount of peak-to-peak craniocaudal tumor motion ranged from 1.2 to 2.5 cm, much larger than the observed amount of anteroposterior tumor motion (see Table 1). The period of breathing motion ranged from 2.7 to 4.5 seconds, and the frequency of motion for the external and internal markers also agreed well, as shown in Fig. 1 for Patient 1 and in Fig. 8 for the remaining 3 patients. Although the motion of the external markers and tumor markers correlated reasonably well, several issues were noted that should be considered when relying solely on external markers as surrogates for tumor motion. Variability in the tumor position, for a given marker position in the respiratory trace, was observed. For 2 patients (Patients 2 and 4), the range in tumor positions for a given marker position was small, about 2 to 3 mm. For the other 2 patients, however, the tumor positions varied by as much as 6 mm (Patient 1) or 9 mm (Patient 3). These results depended on which external marker was observed; that is, the position of the external marker on the patient surface may impact the underlying variation in tumor position relative to the external marker. Also, although data are limited in this study, the markers that moved much less than the tumor tended to have a larger variation in tumor position for

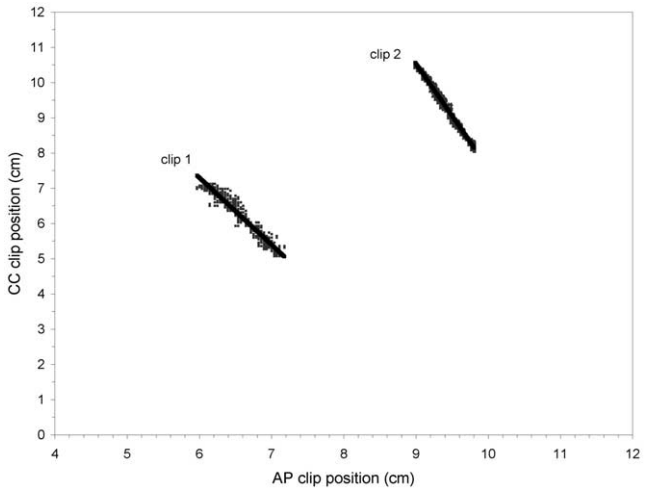

Fig. 5. Craniocaudal (CC) tumor motion vs. anteroposterior (AP) tumor motion for Patient 3.

a fixed marker position. For example, the ratio of tumor motion to external-marker motion was a factor of 7 for Patient 3, and the tumor position varied by as much as 9 mm for a given external-marker position. The potential range of tumor positions for a given marker position is important for respiratory gating because the linear accelerator is gated on or off on the basis of the external-marker position. Any variations in underlying tumor motion not accounted for when designing the gating window could impact the dose coverage of the tumor.

Phase shifts between abdominal tumors and external markers placed on the abdomen were not observed in this study. Ozhasoglu (13) observed phase differences between the chest wall and abdomen surface, as well as between chest displacement and lung tidal volumes, but does not mention phase differences between the abdominal surface and a pancreas tumor. Phase differences have also been shown to vary on the basis of the position of the external marker (7). Furthermore, some patients may breathe with large chest excursions, whereas others may be predominantly abdominal breathers. The anatomic relationship between lung/chest motion and abdominal-surface motion is potentially much more complex than local motion in the abdomen, where the tissue is more continuous and the two observed quantities are closer to each other. Furthermore, the data from Fig. 5 show that the craniocaudal and anteroposterior clip positions are in phase with each other for Patient 3, who had the greatest extent of tumor motion. Any gating window designed to minimize tumor motion in one direction would, therefore, also minimize tumor motion in the other direction.

These results indicate that the location of the external marker is important, as it may affect the variability of tumor position relative to the external marker, as well as impacting the ratio of tumor-to-marker motion. In gathering motion data for gating studies, monitoring the position of multiple external markers relative to the tumor may be useful. Once

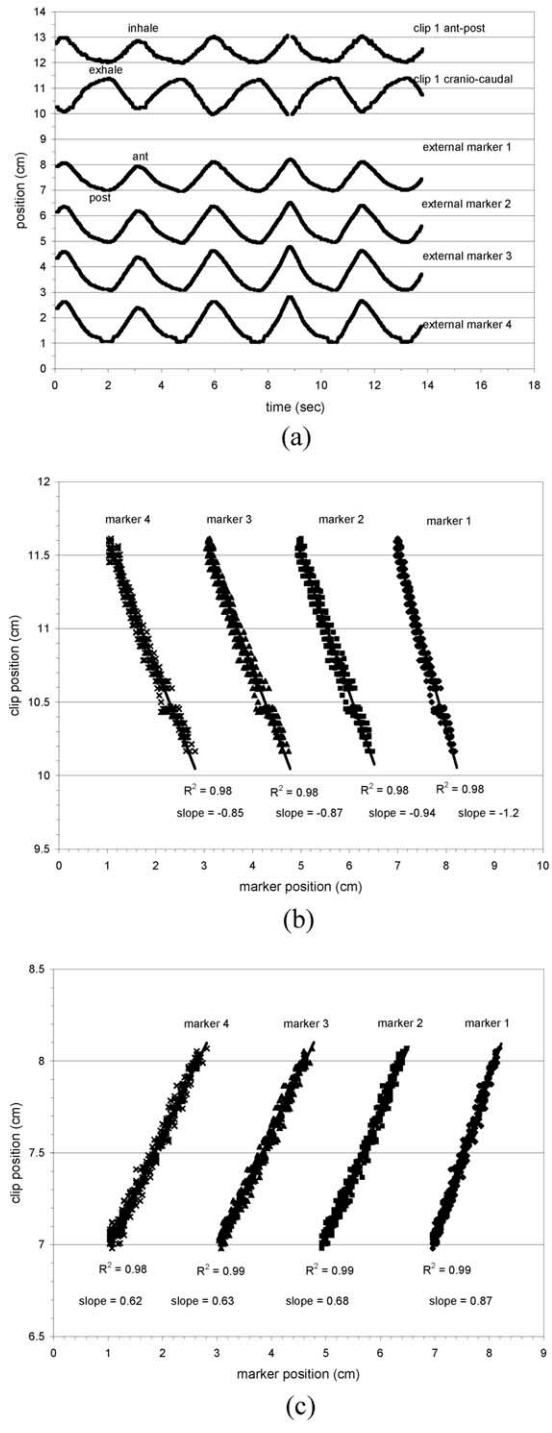

Fig. 6. Patient 4: (a) Craniocaudal and anteroposterior tumor-clip motion and anteroposterior external-marker motion as a function of time. (b) Craniocaudal tumor-clip position as a function of anteroposterior external-marker position. (c) Anteroposterior tumor-clip position as a function of anteroposterior external-marker position. For (a) and (b), the absolute values of the motion traces have been modified for display purposes.

an optimal marker position on the patient is chosen, it should be used throughout the treatment for the best consistency in the gating window. The data in this study were accumulated only for a single day; the daily variation in the

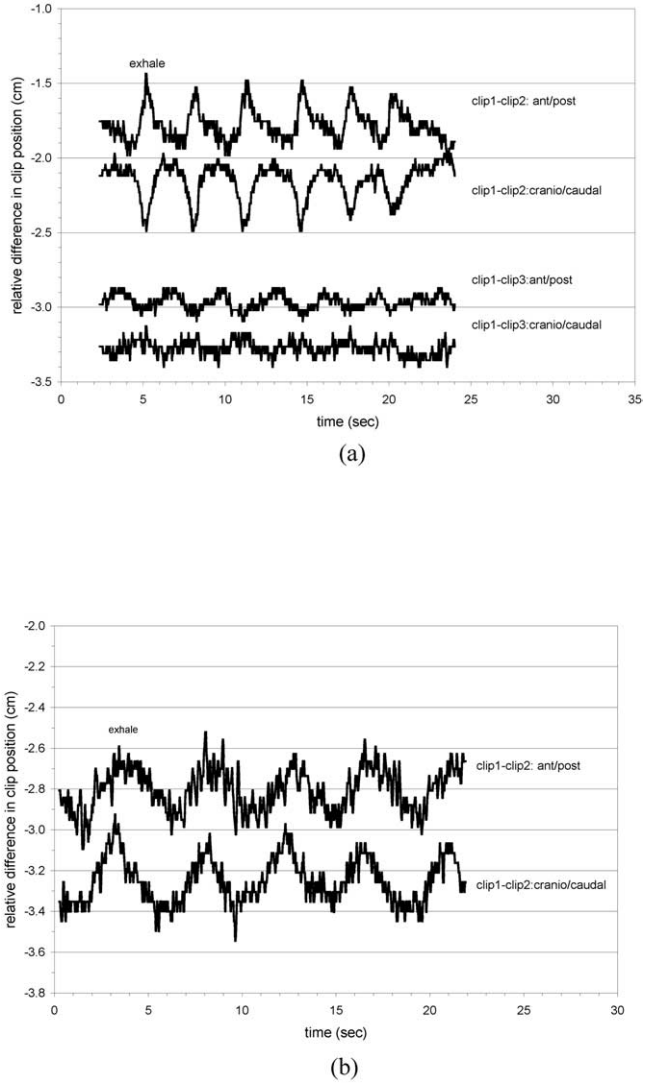

Fig. 7. Difference in clip positions for (a) Patient 2 and (b) Patient 3.

correlation between internal and external motion is currently being studied.

The deformation of the tumor was examined very simply by quantifying the change in the relative spacing of the tumor markers for 2 patients with multiple markers. The relative spacing of the tumor clips varied by as much as 5 mm, and varied according to the position in the breathing cycle with a standard deviation of about 6%, as normalized by the maximum peak-to-peak motion. Although some degree of deformation is certainly observed, the amount of deformation is difficult to fully understand by use of this metric.

This study utilized fluoroscopy to visualize tumor fiducials, which allowed motion data to be gathered continuously over many breathing cycles. Fluoroscopy could also be used in conjunction with four-dimensional CT (4D CT), which can provide detailed motion and anatomic information averaged over 1 breathing cycle. Reitzel (16) has shown

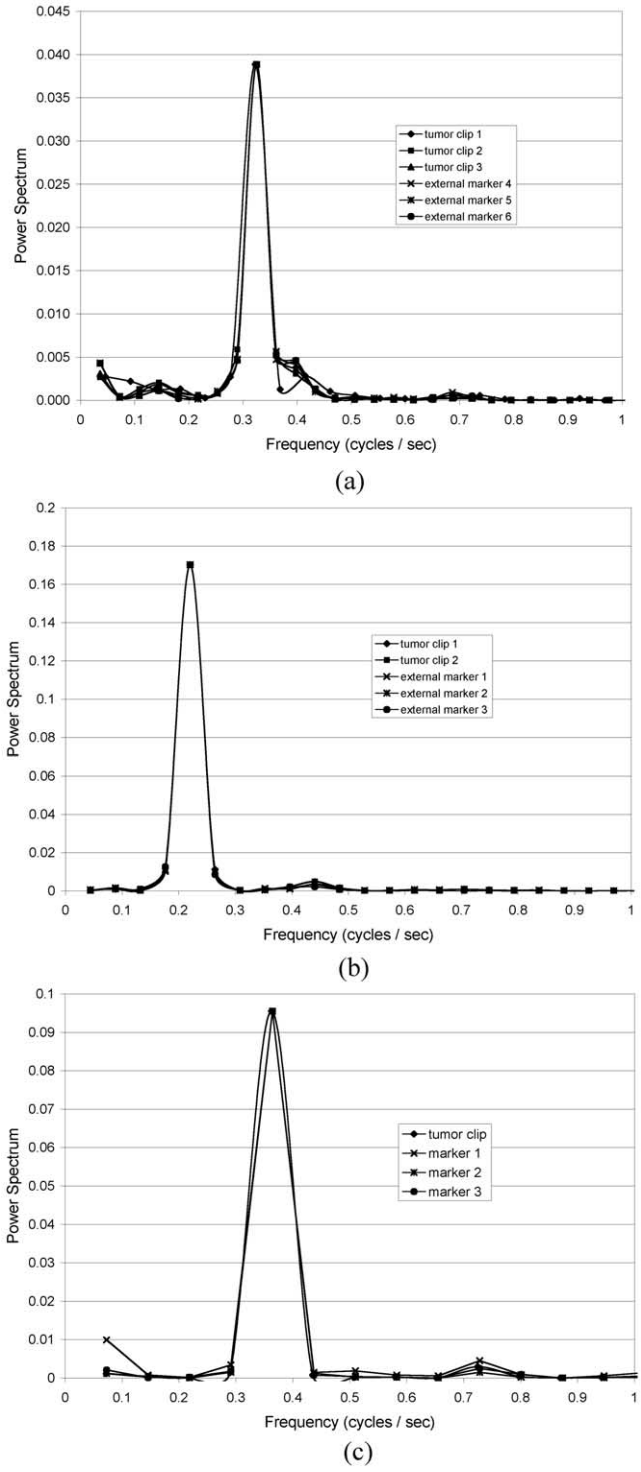

Fig. 8. Power spectrum of tumor clips and external markers for (a) Patient 2, (b) Patient 3, and (c) Patient 4.

reasonable agreement between 4D CT and fluoroscopic analysis of tumor motion.

CONCLUSIONS

This study suggests, on the basis of a limited set of abdominal tumor patients, that tumor motion generally cor-

relates well with external fiducial markers. Potential exists for variations in tumor position for given marker positions, which may degrade the accuracy of the gating window. Treatment margins should be determined on the basis of a detailed understanding of tumor motion, as opposed to relying only on external-marker information.

REFERENCES

1. Langen KM, Jones DTL. Organ motion and its management. *Int J Radiat Oncol Biol Phys* 2001;50:265–278.
2. Suramo I, Paivansalo M, Myllyla V. Cranio-caudal movements of the liver, pancreas and kidneys in respiration. *Acta Radiologica Diagn* 1984;25:129–131.
3. Bryan PJ, Custar S, Haaga JR, *et al.* Respiratory movement of the pancreas: An ultrasonic study. *J Ultrasound Med* 1984;3: 317–320.
4. Brock KK, Hollister SJ, Dawson LA, *et al.* Creating a 4D model of the liver using finite element analysis. *Med Phys* 2002;29:1403–1405.
5. Ohara K, Okumura T, Akisada T, *et al.* Irradiation synchronized with respiration gate. *Int J Radiat Oncol Biol Phys* 1989;17:853–857.
6. Mageras G, Torke E, Rosenzweig KE, *et al.* Fluoroscopic evaluation of diaphragmatic motion reduction with a respiratory gated radiotherapy system. *J Appl Clin Med Phys* 2001; 2:191–200.
7. Vedam SS, Keall PJ, Kini VR, *et al.* Determining parameters for respiration-gated radiotherapy. *Med Phys* 2001;28:2139–2146.
8. Kubo HD, Hill BC. Respiration gated radiotherapy treatment: A technical study. *Phys Med Biol* 1996;41:83–91.
9. Wagman R, Yorke E, Ford E, *et al.* Respiratory gating for liver tumors: Use in dose escalation. *Int J Radiat Oncol Biol Phys* 2003;55:659–658.
10. Ford EC, Mageras GS, Yorke E, *et al.* Evaluation of respiratory movement during gated radiotherapy using film and electronic portal imaging. *Int J Radiat Oncol Biol Phys* 2002;52: 522–531.
11. Shirato H, Shimizu S, Kunieda T, *et al.* Physical aspects of a real-time tumor-tracking system for gated radiotherapy. *Int J Radiat Oncol Biol Phys* 2000;48:1187–1195.
12. Vedam SS, Kini VR, Keall PJ, *et al.* Quantifying the predictability of diaphragm motion during respiration with a noninvasive external marker. *Med Phys* 2003;30:505–513.
13. Ozhasoglu C, Murphy MJ. Issues in respiratory motion compensation during external beam radiotherapy. *Int J Radiat Oncol Biol Phys* 2002;52:1389–1399.
14. Gierga DP, Chen GTY, Kung JH, *et al.* Quantification of respiration-induced abdominal tumor motion and its impact on IMRT dose distributions. *Int J Radiat Oncol Biol Phys* 2004; 58:1584–1595.
15. Betke M, Makris NC. Recognition and complexity of objects subject to affine transformation. *Int J Comput Vis* 2001;44:5–40.
16. Rietzel E, Rosenthal SJ, Gierga DP, *et al.* Moving targets: Detection and tracking of internal organ motion for treatment planning and patient setup. *Radiother Oncol* 2005; In press.